Solid-State Electronics 197 (2022) 108460

Contents lists available at ScienceDirect

Solid State Electronics

journal homepage: www.elsevier.com/locate/sse

Ab initio quantum transport simulations of monolayer GeS nanoribbons

Mislav Matić, Mirko Poljak *

Computational Nanoelectronics Group, Micro and Nano Electronics Laboratory, Faculty of Electrical Engineering and Computing, University of Zagreb, Zagreb HR 10000, Croatia

ARTICLE INFO

Keywords:
Quantum transport
non-equilibrium Green's function (NEGF)
Density functional theory (DFT)
Maximally-localized Wannier functions (MLWF)
GeS
Nanoribbon

ABSTRACT

Monolayer germanium monosulfide (GeS) was recently identified as one of the most promising 2D materials for ultra-scaled FETs. While sub-10 nm monolayer GeS FETs were studied by quantum transport, very little is known about GeS nanoribbons (GeSNRs) or GeSNR FET performance. In this work, we employ quantum transport and Hamiltonians with an orbital resolution to study the electronic, transport, and ballistic device properties of sub-4 nm-wide and ~15 nm-long GeSNRs. While ultra-scaled GeSNR FETs exhibit I_{ON}/I_{OFF} of at least $\sim 7\times10^5$, indicating good switching performance, they also offer modest ballistic I_{ON} values of up to ~1.2 mA/μm.

1. Introduction

Miniaturization and optimization of transistors have driven the tremendous development of the semiconductor industry in the last 60 years. Short channel effects (SCEs) suppression at gate lengths under ~20 nm is difficult and, on that account, new materials and device architectures are needed to enable further transistor scaling and improve device performance. Potential candidates for future transistor channel materials are atomically thin 2D materials (2DMs). Due to their atomic thickness and dangling-bond-free surfaces, 2DMs have high immunity to SCEs, and the near-ballistic transport properties are promising for high-performance devices [1], but the high contact resistance still remains a limiting factor for 2DMs application in nanodevices [2,3]. Patterning 2DMs into quasi–1D nanoribbons enables tuning of the electronic, transport, and device properties [4,5] such as bandgap, effective mass, injection velocity, etc., which makes these nanostructures of interest for nanoelectronic devices.

Monolayer germanium monosulfide (GeS) is a group-IV monochalcogenide 2D material with a buckled orthorhombic lattice. Monolayer GeS was recently examined along with hundreds of 2D materials as one of the most promising 2D materials for ultra-scaled FETs in [1], while a quantum transport study of sub-10 nm monolayer GeS FETs was reported in [6]. On the other hand, very little is known about GeS nanoribbons (GeSNRs) or GeSNR device performance, with the knowledge on the former being limited to electronic properties only, as reported in [7]. Concerning their electronic properties, armchair and zigzag GeSNRs were studied with armchair 2D GeS showing more promise for device applications due to lower electron and hole effective masses. Hence, in this work, we analyze GeSNRs with armchair edges.

Advanced modeling is needed for the simulation of transistors at the nanoscale due to the atomistic resolution of the material and strong quantum effects. Here we use *ab initio* density functional theory (DFT) to perform electronic structure calculations and maximally localized Wannier functions (MLWFs) are employed to transform DFT Hamiltonians into a localized basis, which preserves bandstructure accuracy and reduces the computational load for transport calculations. Next, non-equilibrium Green's function (NEGF) formalism, including the MLWF Hamiltonians, is used for ballistic quantum transport simulations [8–10]. In this work, our in-house DFT-MLWF-NEGF solver is employed to analyze the electronic, transport, and ballistic device properties of ultra-scaled armchair GeSNRs and GeSNR FETs that exhibit a direct bandgap for narrowest nanoribbons.

1.1. Methodology

The unit cell of the 2D GeS is obtained from the 2D materials database provided by Materials Cloud [11], which is then used to construct an armchair GeSNR super-cell along the nanoribbon width (*W*). Edges of the GeSNRs are passivated with H atoms and a vacuum of 20 Å is added in the confined directions to exclude any interactions (existing due to DFT that assumes periodicity in all three directions). We construct and perform DFT simulations for GeSNR super-cells for nanoribbon widths

* Corresponding author.
E-mail address: mirko.poljak@fer.hr (M. Poljak).

https://doi.org/10.1016/j.sse.2022.108460

Available online 16 September 2022

from $W = 0.76$ nm to $W = 3.70$ nm. The DFT calculations are used to relax H-passivated GeSNRs structures and obtain the band structure with high accuracy. Plane-wave based Quantum Espresso program package [12] is used for DFT calculations, with Perdew-Burke-Ernzerhof generalized gradient approximation (PBE-GGA) [13] for the exchange-correlation (XC) functional. The plane-wave cutoff energy is set to 100 Ry, while the convergence threshold is set to 10^{-3} eV/Å for the ionic force, and to the value of 10^{-4} eV for energy. The k-points are sampled using an equally-spaced Monkhorst-Pack grid [14] in the transport direction and 1 k-point in the confined directions. The output of the DFT are dense Hamiltonians localized in energy, but NEGF simulations prefer spatially localized Hamiltonians. Maximally-localized Wannier functions (MLWFs) [15] are used to transform DFT Hamiltonians into a localized basis, which results in much sparser matrices and enables the simulation of devices consisting of thousands of atoms [8,16]. Wannier90 program package [17] is used to obtain the MLWF Hamiltonians. The MLWFs accuracy greatly depends on trial orbitals that are projected on the Bloch manifold. For GeSNRs we choose s, p_x, p_y, and p_z atomic orbitals as trial orbitals for both Ge and S atoms. The MLWF Hamiltonian matrices are then used to construct the total GeSNR channel Hamiltonians of ~15 nm long nanoribbons with different GeSNR widths.

Non-equilibrium Green's function (NEGF) formalism is used to directly solve the Schrödinger's equation with open boundary conditions (OBCs). Retarded Green's function, G^R, of the device is the central quantity of NEGF formalism and can be written as.

$$G^R(E) = [(E + i\eta)I - H - \Sigma_S^R(E) - \Sigma_D^R(E)]^{-1},$$

where H is the total GeSNR channel Hamiltonian, Σ matrices denote source (S) and drain (D) retarded contact self-energies that account for OBCs, and $i\eta$ is the infinitesimal positive imaginary convergence constant used to ensure the physically relevant causal result. The NEGF framework is implemented in our in-house code [4,5,10] which is used for the calculation of size-dependent properties of GeSNRs. Contacts are assumed to be ideal, i.e. semi-infinite regions made up of the same material as the channel, with the Sancho-Rubio method [18] employed for a numerically-efficient calculation of S/D contact self-energy matrices.

Electronic and transport properties are calculated using NEGF, including S/D transmission (T_{SD}) and density of states (DOS), which are used within the top-of-the-barrier (ToB) model [19] to study the ballistic performance of n-channel GeSNR MOSFETs. The ToB model provides the thermionic current and the calculations depend on the self-consistent ToB potential that represents the S/D barrier height, source and drain Fermi-Dirac functions, and Fermi levels for charge neutrality in S/D regions, DOS and T_{SD}. Since only the thermionic current above the ToB potential is calculated, the ToB model is a dependable method for FETs with channel lengths >15 nm where direct S/D tunneling is negligible [19]. Gate oxide has EOT = 1 nm, and S/D doping is set at 0.001 M fraction of the GeS areal density. In all devices, we set a common V_{TH} of 0.24 V as projected in the International Roadmap for Devices and Systems (IRDS) at the "3 nm" logic node [20]. In turn, this V_{TH} results in a very low OFF-state current (I_{OFF}) of 0.87 nA/μm due to the 60 mV/dec subthreshold slope and ideal gate control over the channel that are assumed in the ToB model. The ballistic ON-state current (I_{ON}) is extracted at $V_{GS} = V_{DS} = 0.7$ V, i.e. when both gate and drain are biased at the supply voltage.

2. Results and discussion

Fig. 1 shows the top (Fig. 1a) and side (Fig. 1b) view of a relaxed 1.86 nm-wide armchair GeS nanoribbon structure passivated with H atoms. GeS exhibits buckled orthorhombic structure and after relaxation, a slight shift of the edge Ge and S atoms are observed and visible in Fig. 1a. In Fig. 2 bandgap is shown for various nanoribbon widths. Scaling down nanoribbon width increases the bandgap (E_g) from 1.73 eV

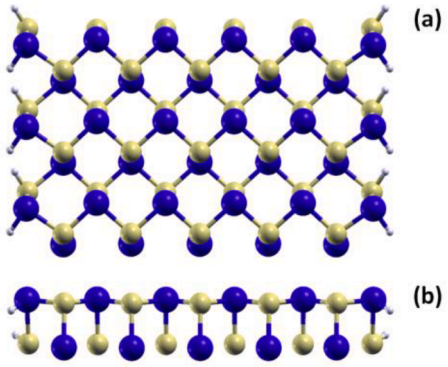

Fig. 1. (a) Top and (b) side view of the monolayer GeS nanoribbon with armchair edges.

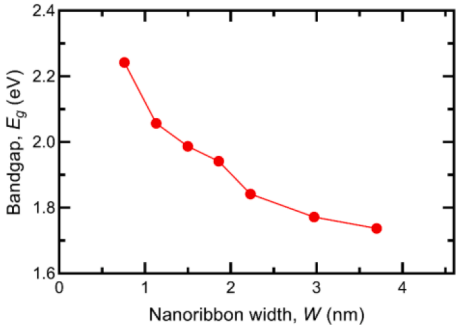

Fig. 2. Impact of width-scaling on the bandgap of armchair GeSNRs.

for $W = 3.70$ nm to 2.24 eV for $W = 0.76$ nm. The bandstructure plots for GeSNRs of various widths, reported in Fig. 3, show that E_g of wider GeSNRs is indirect while scaling down the nanoribbon width below $W =$ 2.23 nm transitions GeSNRs into a direct semiconductor which agrees with the results in [7]. Effective mass (m^*, in units of m_0) of the lowest conduction band is calculated and reported in Fig. 3. Effective mass increases while scaling down nanoribbon width from $m^* = 0.276$ for W = 3.70 nm to $m^* = 1.143$ for $W = 0.76$ nm. The effective mass is high even for the widest nanoribbons when compared to m^* of the lowest conduction band in 2D GeS alongside armchair direction ($m^* = 0.2$ was reported in [21]). In Fig. 4 the width-dependence of the ON-state current for armchair GeSNR MOSFETs is shown. The ON-state current decreases monotonically while scaling down the GeSNR width, from $I_{ON} = 1.20$ mA/μm for $W = 3.70$ nm to $I_{ON} = 0.65$ mA/μm for $W = 0.76$ nm. The performance of GeSNR FETs is directly related to the channel bandstructure along nanoribbon transport direction, as reported in Fig. 3 since mobile charge density depends on the density of states (DOS), and the transmission function determines transport probability for each conducting mode. Subbands nearest to the conduction band minimum (CBM) have the highest influence on the ON-state current in n-channel FETs. For nanoribbons with $W = 2.97$ nm and $W = 3.70$ nm, I_{ON} values are approximately the same due to bandstructure similarity near the CBM for both GeSNRs. To further clarify the $I_{ON} - W$ curve, transmission and DOS are plotted in the ~200 meV energy range from the CBM, with CBM shifted to 0 eV for an easier comparison of different GeSNRs as shown in Fig. 5. Nanoribbons with $W = 3.70$ nm and $W = 2.97$ nm show DOS and transmission characteristics that match almost perfectly for energies up to 0.11 eV away from the CBM, where the contribution to the current is the highest, thus resulting in the same I_{ON}. The 2.23 nm-wide GeSNR presents a transitional nanoribbon because the lowest sub-bands nearest to the CBM start moving away from the CBM as W decreases further (e.g. compare Fig. 3c and d). This subband shift directly translates into the significant I_{ON} drop while scaling the GeSNR

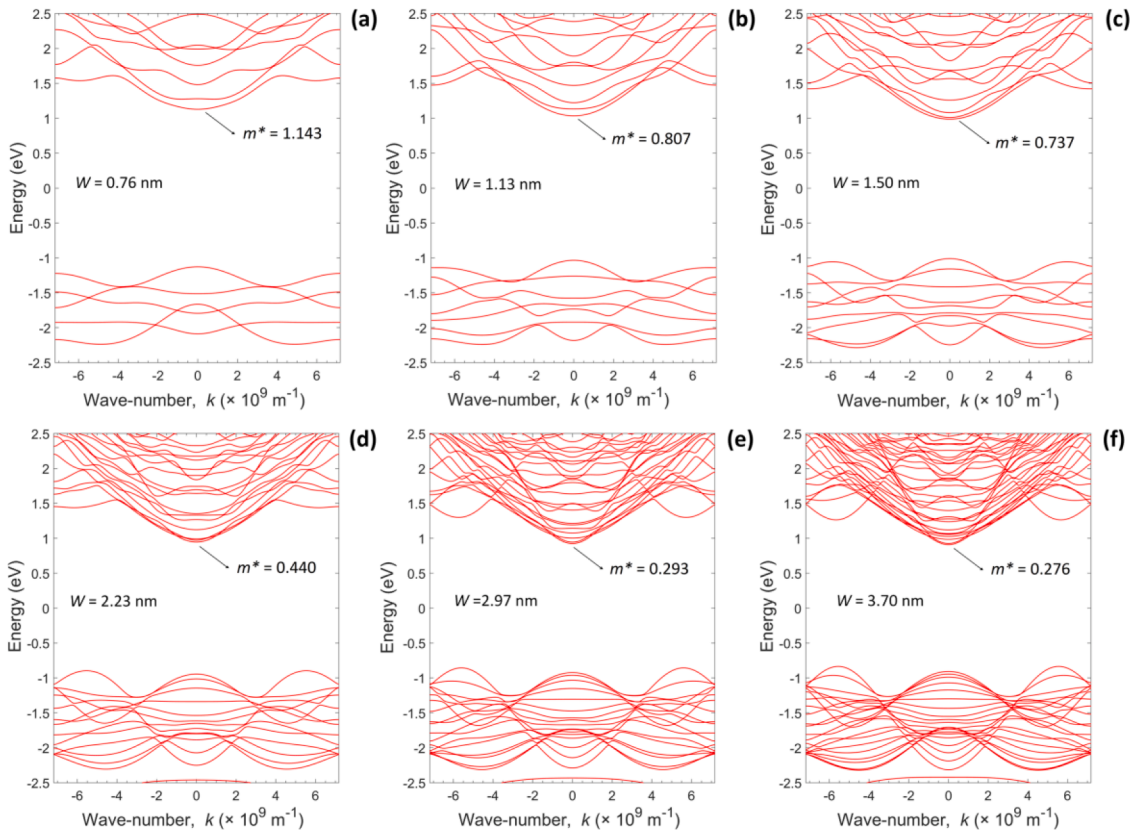

Fig. 3. Bandstructure of GeSNRs with the widths of (a) W = 0.76 nm, (b) W = 1.13 nm, (c) W = 1.50 nm, (d) W = 2.23 nm, (e) W = 2.97 nm, and (f) W = 3.70 nm with extracted effective mass (in units of m_0) of electrons in the lowest conduction band.

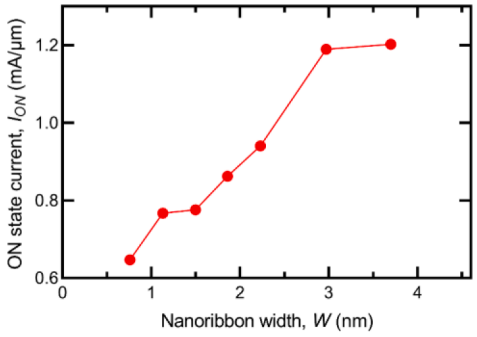

Fig. 4. Width-dependence of the ON-state current extracted at 0.7 V supply voltage in armchair GeSNR FETs.

width from 2.97 nm to 2.23 nm observed in Fig. 4. For GeSNRs with W <2.23 nm the subband with lower curvature, i.e. higher effective mass, becomes the lowest subband that dominantly determines the overall transport. This property, alongside the lower number of available bands/modes due to the lower number of available orbitals in narrower GeSNRs, further decreases I_{ON} in ultra-scaled GeSNR FETs. None of the analyzed devices fulfills IRDS specification for I_{ON} at the "3 nm" node, but the ON-state performance can be somewhat improved by optimizing the EOT, doping, etc., which is beyond the scope of this work. On the other hand, I_{ON}/I_{OFF} reaches ~7×10^5 even in the worst case, indicating good switching capabilities of GeSNR FETs for logic applications.

3. Conclusions

We employ NEGF with MLWF Hamiltonians to study the electronic, transport and ballistic device properties of sub-4 nm-wide and ~15 nm-

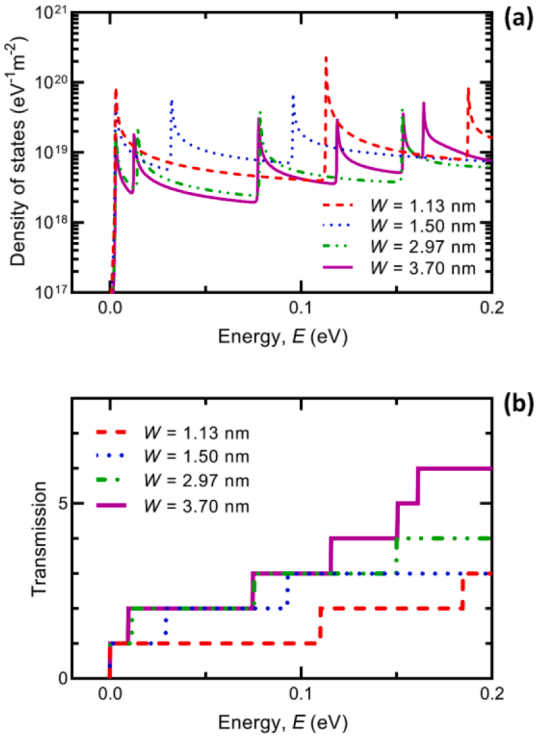

Fig. 5. (a) Density of states and (b) transmission comparison for armchair GeSNRs with the widths of W = 1.50 nm (dotted blue line), W = 1.86 nm (dashed red line), W = 2.97 nm (dot-dot-dashed green line), and W = 3.70 nm (purple line). (For interpretation of the references to colour in this figure legend, the reader is referred to the web version of this article.)

long GeSNRs. The I_{ON}/I_{OFF} ratio of at least $\sim 7\times10^5$ is observed for ultra-scaled GeSNR FETs, which indicates good switching performance for digital logic devices. The ON-state performance deteriorates as the GeSNR width is scaled down, with the maximum ballistic I_{ON} of ~1.20 mA/μm achieved for the widest analyzed GeSNR FET with $W = 3.70$ nm. While GeSNR FETs do not meet the IRDS requirements at the "3 nm" CMOS node and beyond, further performance improvement of GeS-based nanodevices is possible by doping and gate-stack engineering. Nevertheless, future work must also consider carrier scattering and dissipative transport for a realistic assessment. [9].

Declaration of Competing Interest

The authors declare that they have no known competing financial interests or personal relationships that could have appeared to influence the work reported in this paper.

Data availability

Data will be made available on request.

Acknowledgments

This work was supported by the Croatian Science Foundation under the project CONAN2D (Grant No. UIP-2019-04-3493).

References

[1] Klinkert C, Szabó Á, Stieger C, Campi D, Marzari N, Luisier M. 2-D Materials for Ultrascaled Field-Effect Transistors: One Hundred Candidates under the *Ab Initio* Microscope. ACS Nano Jul. 2020;14(7):8605–15. https://doi.org/10.1021/acsnano.0c02983.

[2] Poljak M, Matic M, Zeljko A. Minimum Contact Resistance in Monoelemental 2D Material Nanodevices with Edge-Contacts. IEEE Electron Device Lett 2021;42(8):1240–3.

[3] Allain A, Kang J, Banerjee K, Kis A. Electrical contacts to two-dimensional semiconductors. Nature Mater 2015;14(12):1195–205.

[4] Poljak M. Electron Mobility in Defective Nanoribbons of Monoelemental 2D Materials. IEEE Electron Device Lett 2020;41(1):151–4.

[5] Poljak M, Matić M. Bandstructure and Size-Scaling Effects in the Performance of Monolayer Black Phosphorus Nanodevices. Materials Dec. 2021;15(1):243. https://doi.org/10.3390/ma15010243.

[6] Ding Y, et al. High-Performance Ballistic Quantum Transport of Sub-10 nm Monolayer GeS Field-Effect Transistors. ACS Appl Electron Mater Mar. 2021;3(3):1151–61. https://doi.org/10.1021/acsaelm.0c01019.

[7] Li R, Cao H, Dong J. Electronic properties of group-IV monochalcogenide nanoribbons: Studied from first-principles calculations. Phys Lett A Nov. 2017;381(44):3747–53. https://doi.org/10.1016/j.physleta.2017.09.048.

[8] Klimeck G, Luisier M. Atomistic Modeling of Realistically Extended Semiconductor Devices with NEMO and OMEN. Comput Sci Eng Mar. 2010;12(2):28–35. https://doi.org/10.1109/MCSE.2010.32.

[9] A. Afzalian and G. Pourtois, "ATOMOS: An ATomistic MOdelling Solver for dissipative DFT transport in ultra-scaled HfS $_2$ and Black phosphorus MOSFETs," in *2019 International Conference on Simulation of Semiconductor Processes and Devices (SISPAD)*, Udine, Italy, Sep. 2019, pp. 1–4. 10.1109/SISPAD.2019.8870436.

[10] M. Matić, T. Župančić, and M. Poljak, "Parallelized Ab Initio Quantum Transport Simulation of Nanoscale Bismuthene Devices," in *2022 45th Jubilee International Convention on Information, Communication and Electronic Technology (MIPRO)*, 2022, pp. 118–123. 10.23919/MIPRO55190.2022.9803335.

[11] Talirz L, Kumbhar S, Passaro E, Yakutovich AV, Granata V, Gargiulo F, et al. Materials Cloud, a platform for open computational science. Sci Data 2020;7(1).

[12] Giannozzi P, Baroni S, Bonini N, Calandra M, Car R, Cavazzoni C, et al. QUANTUM ESPRESSO: a modular and open-source software project for quantum simulations of materials. J Phys: Condens Matter 2009;21(39):395502.

[13] Perdew JP, Burke K, Ernzerhof M. Generalized Gradient Approximation Made Simple. Phys Rev Lett 1996;77(18):3865–8.

[14] Monkhorst HJ, Pack JD. Special points for Brillouin-zone integrations. Phys Rev B 1976;13(12):5188–92.

[15] Marzari N, Vanderbilt D. Maximally localized generalized Wannier functions for composite energy bands. Phys Rev B 1997;56(20):12847–65.

[16] Calderara M, Brück S, Pedersen A, Bani-Hashemian MH, VandeVondele J, Luisier M. Pushing back the limit of ab-initio quantum transport simulations on hybrid supercomputers. In: Proceedings of the International Conference for High Performance Computing, Networking. Austin Texas: Storage and Analysis; 2015. p. 1–12. https://doi.org/10.1145/2807591.2807673.

[17] Pizzi G, Vitale V, Arita R, Blügel S, Freimuth F, Géranton G, et al. Wannier90 as a community code: new features and applications. J Phys: Condens Matter 2020;32(16):165902.

[18] Sancho MPL, Sancho JML, Rubio J. Quick iterative scheme for the calculation of transfer matrices: application to Mo (100). J Phys F: Met Phys 1984;14(5):1205–15.

[19] A. Rahman, Jing Guo, S. Datta, and M. S. Lundstrom, "Theory of ballistic nanotransistors," *IEEE Trans. Electron Devices*, vol. 50, no. 9, pp. 1853–1864, Sep. 2003, 10.1109/TED.2003.815366.

[20] '"IEEE Intl. Roadmap for Devices and Systems (IRDS), 2019 Update.' https://irds.ieee.org/.".

[21] Li F, Liu X, Wang Y, Li Y. Germanium monosulfide monolayer: a novel two-dimensional semiconductor with a high carrier mobility. J. Mater. Chem. C 2016;4:2155–9. https://doi.org/10.1039/C6TC00454G.